

Mol Pharm. Author manuscript; available in PMC 2011 February 1.

Published in final edited form as:

Mol Pharm. 2010 February 1; 7(1): 291. doi:10.1021/mp900245h.

Stabilization of the Nitric Oxide (NO) Prodrugs and Anti-Cancer Leads, PABA/NO and Double JS-K through Incorporation into PEG-Protected Nanoparticles

Varun Kumar[†], Sam Y. Hong[§], Anna E. Maciag[‡], Joseph E. Saavedra[‡], Douglas H. Adamson[¶], Robert K. Prud'homme^{†,*}, Larry K. Keefer[§], and Harinath Chakrapani^{T,*}

[†]Department of Chemical Engineering, Princeton University, Princeton, New Jersey 08544

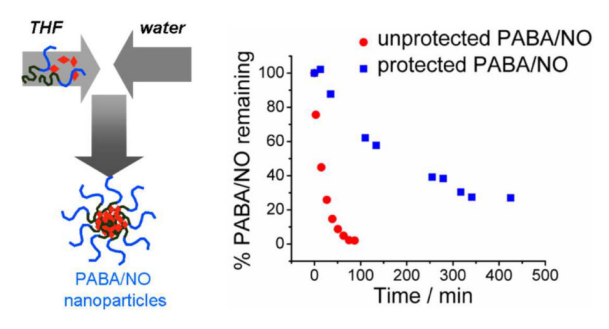
§Chemistry Section, Laboratory of Comparative Carcinogenesis, National Cancer Institute at Frederick, Frederick, Maryland 21702

[‡]Basic Science Program, SAIC-Frederick, National Cancer Institute at Frederick, Frederick, Maryland 21702

[¶]Department of Chemistry and Institute for Material Science, University of Connecticut, Storrs, Connecticut 06269

^TDepartment of Chemistry, Indian Institute of Science Education and Research, Pune 411008, India

Abstract



Here we report the stabilization of the nitric oxide (NO) prodrugs and anti-cancer lead compounds, PABA/NO (O^2 -{2,4-dinitro-5-[4-(N-methylamino)benzoyloxy]phenyl} 1-(N,N-dimethylamino) diazen-1-ium-1,2-diolate) and "Double JS-K" (1,5-bis{[1-[(4-ethoxycarbonyl)piperazin-1-yl] diazen-1-ium-1,2-diol-2-ato]-2,4-dinitrobenzene), through their incorporation into polymer-protected nanoparticles. The prodrugs were formulated in block copolymer-stabilized nanoparticles with sizes from 220 to 450 nm by a novel rapid precipitation process. The block copolymers, with polyethylene glycol (PEG) soluble blocks, provide a steric barrier against NO prodrug activation by glutathione. Too rapid activation and NO release has been a major barrier to effective administration of this class of compounds. The nanoparticle stabilized PABA/NO from attack by glutathione as evidenced by a significant increase in time taken for 50% decomposition from 15 min (unformulated) to 5 h (formulated); in the case of Double JS-K, the 50% decomposition time was extended from 4.5 min (unformulated) to 40 min (formulated). The more hydrophobic PABA/NO produced more stable nanoparticles and correspondingly more extended release times in comparison with Double JS-K. The hydrophobic blocks of the polymer were either polystyrene or polylactide. Both blocks produced nanoparticles of approximately the same size and release kinetics. This combination of PEG-

protected nanoparticles with sizes appropriate for cancer targeting by enhanced permeation and retention (EPR) and delayed release of NO may afford enhanced therapeutic benefit.

Keywords

Nitric oxide; PABA/NO; glutathione; glutathione S-transferase; nanoparticles; formulation

INTRODUCTION

Nitric oxide (NO) is a mediator of diverse physiological processes and has been shown to have anti-proliferative activity. ^{1–3} Due to the poor bioavailability of NO, typically prodrugs of nitric oxide such as diazeniumdiolates are used as surrogates of NO. ⁴ O²-(2,4-Dinitrophenyl) diazeniumdiolates are important members of the diazeniumdiolate class of nitric oxide prodrugs that have shown promising anti-cancer activity. ⁵ Some important examples are JS-K (*O*²-(2,4-dinitrophenyl) 1-[(4-ethoxycarbonyl)piperazin-1-yl]diazen-1-ium-1,2-diolate) ^{6–15} and PABA/NO, ^{16–22} which have both shown potent tumoristatic effects in animal models (Figure 1). For example, JS-K was found to inhibit the *in vivo* growth of xenografts of cells derived from human leukemia, multiple myeloma, and prostate carcinoma. PABA/NO showed tumoristatic activity against A2780 human ovarian cancer xenografts in female SCID mice with a potency comparable to that of cisplatin.

The general mechanism of activation of such prodrugs involves a nucleophilic aromatic substitution by glutathione (GSH) followed by spontaneous decomposition of the ensuing diazeniumdiolate anion to generate nitric oxide under physiological conditions (Scheme 1).⁵ The aforementioned reaction was found to be catalyzed by glutathione *S*-transferase (GST), a class of detoxification enzymes that is frequently over-expressed in cancers.^{14, 21}

Double JS- K^{12} (Figure 1) is a second-generation JS-K analogue that was designed to generate up to 4 moles of NO per mole of compound and has shown potent in vitro anti-proliferative effects against human leukemia cells. ¹⁷

As JS-K and PABA/NO react with glutathione even in the absence of GST, our goal during preclinical development of such prodrugs was to minimize reactivity of the prodrug with glutathione in order to increase circulation time and ultimately its efficacy. Our approach towards stabilizing nitric oxide prodrugs was to encapsulate these prodrugs in the form of suitable nanoparticles.

Nanoparticles (NP) have previously been reported as potential delivery vehicles for various therapeutic agents. ^{23–25} Gref et al. ²⁵ reported the advantages of PEGylated polymeric nanoparticles in terms of the circulation time and release of the encapsulated drug. Polyethylene glycol-*b*-poly(lactic-co-glycolic acid) (PEG-*b*-PLGA)-based nanospheres showed longer circulation time and reduced liver uptake compared to PLGA nanospheres with no PEG coating. ²⁵ The concept of a protected prodrug has been widely used to sustain release of cytotoxic agents. Schoenmakers et al. have tailored the cleavage kinetics of ester bonds to control paclitaxel release. ²⁶ The research groups of Baker²⁷ and Kannan^{28, 29} have prepared prodrugs based on dendrimer scaffolds. Sengupta et al. ³⁰ conjugated doxorubicin with PLGA and nucleated the prodrug inside a nanoscale PEGylated phospholipid envelope. The conjugation led to a shift in concentration (~1.8 times) corresponding to half-maximal response. Ansell et al. ³¹conjugated paclitaxel with various lipophilic alcohols to tune the hydrophobicity of the drug and hence its partitioning rate, which directly correlated to efficacy.

In this study, nitric oxide prodrug molecules have been encapsulated into the nanoparticle form and the impact of the polymer protecting layer has been analyzed. The formation and processing of the nanoparticles were observed not to affect the molecular activity of the drug compounds. The formulated nanoparticles of the drug compounds showed significant improvement in stability against glutathione, and a similar anti-proliferative activity as the naked drug molecules.

EXPERIMENTAL SECTION

Materials

The nitric oxide prodrugs JS-K, PABA/NO, and Double JS-K were prepared using previously reported methods. ^{12,19,32} Poloxamer[®] 188 was obtained from BASF Corporation, Parsippany, NJ. Trehalose (D-trehalose dihydrate) was purchased from Sigma-Aldrich Inc., Milwaukee, WI. The stabilizer, poly-L-lactide-*b*-poly (ethylene glycol) (PLA-*b*-PEG, 4.2k-*b*-5k) was purchased from Polymer Source, Inc., Richmond, IN. Polystyrene-*b*-poly (ethylene glycol) (PS-*b*-PEG, 1.5k-*b*-3k) was synthesized by high vacuum anionic polymerization methods ³² using hydroxide capped PS initiated by potassium naphthalenide followed by addition of ethylene oxide.

Nanoparticle formation

Aqueous solution—Poloxamer® 188 and trehalose were dissolved in milli-Q water at the concentration of 9.5 and 12 mg/mL respectively. The aqueous solution was filtered through 0.2- μ m syringe filter (Whatman Inc., Florham park, NJ).

Organic solution—Block copolymer (PS-*b*-PEG or PLA-*b*-PEG) was dissolved in 3.5 mL of tetrahydrofuran, (THF), at the concentration of 8.6 mg/mL. The mixture was sonicated to get a clear solution. NO prodrug (\sim 10.5 mg) was then added to the clear solution. The mixed solution was sonicated and filtered through a 0.2 μ m syringe filter.

Particle Formation—The nanoparticles were produced by a rapid micromixing, rapid precipitation, and block copolymer-directed encapsulation process called Flash NanoPrecipitation (FNP), which is shown schematically in Figure 2. The design and operation of the multi-inlet vortex mixer (MIVM) used to formulate the nanoparticles have been described previously.^{34–38} The organic stream (12 mL/min) was mixed against the aqueous streams (3 streams, each at 40 mL/min) in the MIVM to precipitate the drug followed by stabilization with the block copolymers. The nanoparticle suspension was collected in a 50 mL sterile tube (Becton Dickinson & Co., Franklin lakes, NJ).

Dynamic laser light scattering was used to determine the particle size (expressed as the intensity weighted diameter) with a Zeta sizer (Malvern Instruments, Inc., Westborough, MA). All measurements were made at 532 nm wavelength at the scattering angle of 173° using normal resolution mode as the analysis model.

Processing of nanoparticle dispersion

The nanoparticle dispersion was processed using two different routes: dialysis and lyophilization, to remove the residual organic solvent.

Dialysis—The nanoparticle dispersion was dialyzed against pure water using a Spectra/Por dialysis membrane (Spectrum laboratories, Inc., CA) with a Molecular Weight Cut-Off (MWCO) of 6k-8k Daltons.

Lyophilization—The undialyzed nanoparticle suspension was immediately transferred into a series of 2 mL sterile cryogenic vials (Corning Inc., Corning, NY) dipped into a dry ice/acetone bath to rapidly freeze the sample. The vials were left in the bath for 30–40 min. The vials were lyophilized at -76 °C and 70 mTorr for 3 days. The lyophilized powder was reconstituted in PBS (pH = 7.4) to the desired concentration. 2 mL of PBS was added to each cryogenic vial containing the lyophilized powder and the solution was sonicated with a probe tip sonication for ~3 min at 2–3 watts (Fisher scientific model 100 sonic dismembrator, with a 3.2 mm tip) with the vial dipped in an ice bath to avoid heating during sonication.

Stability Studies

A glutathione stock solution (40 mM) was prepared in 0.1 M phosphate buffer (pH = 7.4). A DMSO stock solution of the prodrug (1 mM) was prepared. To 800 μ L of 0.1 M phosphate buffer (pH = 7.4), 100 μ L of glutathione (40 mM) and 100 μ L of prodrug (1 mM) were added and the disappearance of the prodrug was monitored using an Agilent 1100 series HPLC fitted with a C-18 reverse phase column (Phenomenex Luna 250 × 4.60 mm) operating at 300 nm and run isocratically with acetonitrile:water (75:25). The studies with the nanoparticles were conducted as described above except that the reconstituted nanoparticles were used instead of the DMSO stock solution of the prodrug.

Cell Culture and Cytotoxicity Assays

Human leukemia U937 and human lung cancer H1703 cell lines were obtained from American Type Culture Collection (ATCC, Manassas, VA). Cells were maintained in RPMI 1640 medium (Gibco, Invitrogen, Carlsbad, CA) supplemented with 10% fetal calf serum (Gemini Bio-Products, Sacramento, CA), 100 U/mL penicillin and 2 mM glutamine, at 37 °C and 5% CO2. The CellTiter 96 non-radioactive cell proliferation assay (MTT assay, Promega, Madison, WI), performed according to the manufacturer's protocol, was used to measure cell growth. Cells were seeded in 96-well plates at the density of 10^4 per well and allowed to grow for 24 h before addition of the drugs. Diazeniumdiolate prodrugs were prepared as 10 mM stock solution in DMSO (Sigma, St. Louis, MO). Increasing drug concentrations in $10~\mu$ L of PBS were added to $100~\mu$ L of the culture medium for 72 h. Each compound concentration was represented in six repeats, and the screening was performed as at least two independent experiments. IC50 values were determined using curve fitting algorithm by SigmaPlot (Systat, San Jose, CA).

RESULTS

PABA/NO nanoparticles

Nanoparticles of 240 and 225 nm diameter were obtained for PS-*b*-PEG- and PLA-*b*-PEG-stabilized particles, respectively (Figure 3). A slow increase in size was observed for the undialyzed dispersion during its storage at 4 °C (Figure 3) so that the average particle size grew to 440 nm over 20 h. The process of diffusion-induced growth of particle size is termed Ostwald ripening and has been modeled quantitatively for these polymer-protected nanoparticles. ³⁹ The slow growth resulted in macroscopic precipitation after two to three days. PS-*b*-PEG stabilized PABA/NO nanoparticles were formed with $1\times$ PBS (pH = 7.3) as the aqueous stream. The stability results were qualitatively similar; as 195 nm sized particles at t = 0 h grew to 250 nm over 2.5 h and precipitated over 24 h. The particles in DI water grew in size by 65% over the same period but were more stable after 24 h. The process of particle growth by Ostwald ripening is relatively insensitive to ionic strength.

Dialysis of the nanoparticle dispersion resulted in precipitation in the dialysis membrane within a few hours during dialysis. However, freeze-drying of the sample immediately after formation

led to a stable powder form that could be reconstituted to the original (initial) particle size at the time of administration. Freeze drying also removes the THF co-solvent used in processing.

Double JS-K nanoparticles

Stable nanoparticles of the JS-K drug could not be formed. The product stream from the MIVM immediately precipitated as a macroscopic solid. This lack of protection by the block copolymer during precipitation arises from two effects. First, JS-K was relatively soluble and so the Ostwald ripening kinetics⁴⁰ was rapid and the high surface energy nanoparticles re-form as larger, lower surface area, precipitates. Also, the hydrophobic block of the polymer has a less favorable interaction energy with the more hydrophilic JS-K particle surface. This lack of strong interaction leads to poor coverage and protection by the block copolymer. We have studied this phenomenon in the context of hydrophobic polypeptide nanoparticle formation.

⁴¹ In order to increase the hydrophobicity, Double JS-K was synthesized (Figure 1). ¹²
Nanoparticles formed of Double JS-K with sizes 200 and 195 nm were obtained using PS-b-PEG and PLA-b-PEG as stabilizers, respectively (Figure 4).

Both dialyzed and undialyzed dispersions gave a macroscopic precipitation within a few hours, displaying a higher instability compared to PABA/NO nanoparticles. Figure 4 shows the initial sizes of the Double JS-K nanoparticles and then the particle size for the PS-*b*-PEG-stabilized nanoparticles where the particle size has grown to 290 nm after 1 h. This observation is consistent with the somewhat lower calculated solid phase partition coefficients (i.e. logP) of Double JS-K, logP = 2.12 and PABA/NO, logP = 3.30.⁴² Immediate freeze-drying of the sample was carried out to prepare stable Double JS-K nanoparticle powders.

Since the relevant assays and applications involve time scales of hours, and the release of drug, which is the driver of Ostwald ripening, is the desired outcome of drug delivery, long-term changes in particle size in vitro are not a significant problem. The dispersion from the mixer, with the shown particle distributions, was immediately frozen and lyophilized. Redispersion at the time of use resulted in particle sizes identical to the initial distribution. The molecular activity/effective concentration of the formulated PABA/NO in lyophilized nanoparticle form was compared to the unformulated PABA/NO using UV-absorbance via a UV-vis spectrophotometer (Evolution 300, Thermo Electron Corporation, England). The PABA/NO displays a characteristic absorbance peak at 321 nm. The lyophilized powder was dissolved in THF to yield $\sim 9.4 \times 10^{-3}$ mg/mL PABA/NO and the UV absorbance from the solution was compared with the naked PABA/NO drug solution in THF at $\sim 8.56 \times 10^{-3}$ mg/mL. Absorbance peaks at ~ 321 nm of around the same intensity were observed from both the samples (Figure 5).

Next, these nanoparticles were reconstituted in phosphate buffered saline (PBS, pH 7.4). Based on a calibration curve generated by HPLC analysis of PABA/NO standards, the amount of PABA/NO in the formulation was calculated (Table 1). A similar procedure was carried out for Double JS-K nanoparticles and the recovery of Double JS-K was found to be comparable to that of PABA/NO.

Reaction of Formulated and Unformulated Prodrug with Glutathione

The reaction of PABA/NO with 4 mM glutathione was monitored via HPLC analysis. Under pseudo first-order conditions, a time-dependent disappearance of PABA/NO was observed and a rate constant of $4.6 \times 10^{-2} \, \mathrm{s}^{-1}$ was obtained; the calculated half-life was 15 min (Figure 6).

Under identical reaction conditions, Double JS-K was found to disappear with a half-life of 4.5 min and a pseudo first order rate constant of 0.154 s^{-1} (Figure 7).

Next, the nanoparticle formulations of PABA/NO were tested. In the case of the PS-*b*-PEG-stabilized PABA/NO formulation, roughly 50% of the PABA/NO remained after ~5 h while for PLA-*b*-PEG-stabilized PABA/NO formulation, roughly 50% remained after ~3 h (Figure 8).

Similarly, the formulation was found to protect Double JS-K. The PS-*b*-PEG and PLA-*b*-PEG formulations were similar in behavior: roughly 50% Double JS-K disappeared in 40 min (Figure 9).

Anti-proliferative activity of PABA/NO

The anti-proliferative effects of PABA/NO were determined in two cell lines, human leukemia U937 and human non-small cell lung cancer H1703 cells. Nearly identical IC₅₀ values for formulated and unformulated PABA/NO were obtained (Table 2). A comparison of inhibitory activity of PABA/NO against U937 cells can be found in Figure 10.

DISCUSSION

The encapsulation and NO release of JS-K, Double JS-K, and PABA/NO were consistent with their respective calculated hydrophobicities. The calculated solid phase partition coefficients (i.e. logP) of the compounds are: JS-K, logP = 1.99; Double JS-K, logP = 2.12; and PABA/ NO, logP = 3.30.⁴² Attempts at formulating JS-K into nanoparticle form were unsuccessful due to its relatively higher solubility in aqueous solution. However, the precipitation into nanoparticle form of the more hydrophobic PABA/NO and Double JS-K were successful with both PS-b-PEG and PLA-b-PEG block copolymers. There is little difference in sizes of the nanoparticles produced by either block copolymer, and only a small difference in the release rates of drug from either polymer. The dependence of drug release on the interaction between drug and polymer has been previously studied. A slightly better protection of PABA/NO by PS block (solubility parameter, $\delta_{PS}=18.6~MPa^{1/2}$) as compared to PLA block (solubility parameter, $\delta_{PLA} = 23.3 \text{ MPa}^{1/2})^{42}$ could be due to the stronger interaction between the more hydrophobic PS block and PABA/NO as compared to less hydrophobic PLA. However it might also be related to the higher glass transition temperature of PS $(T_g = 95 \text{ °C})^{40}$ providing higher rigidity on the nanoparticle surface as compared to PLA ($T_g = 60-65$ °C).⁴⁴ But the biodegradability of the PLA block relative to the PS block is probably the most important criterion for selection of the polymer for eventual therapeutic applications. The stability of the Double JS-K nanoparticles was significantly better than that of JS-K because the Ostwald ripening rate depends both on the solubility of the compound⁴⁰ (Double JSK being more hydrophobic) and also upon the diffusion coefficient.³⁹ Double JS-K, being a larger molecule is expected to have a diffusion coefficient approximately 40% smaller than JS-K. Therefore, Double JS-K nanoparticles were sufficiently stable that they could be freeze-dried and administered. The increased rate of glutathione-decomposition of Double JS-K relative to PABA/NO is related to the higher solubility of the Double JS-K which favors dissolution.

CONCLUSIONS

Nitric oxide prodrugs with anti-proliferative activity can be stabilized as nanoparticles with significant protective effects from activation by glutathione. The protection for times of 5–6 hours is believed to be optimal for delivery to solid cancer tumors by the mechanism of enhanced permeation and retention (EPR). 45–47 By this mechanism particles in the size range of 100–300 nm can pass through the defects in the rapidly growing vasculature in tumors and deposit in the tissue. This requires effective passivation of the nanoparticle to prevent premature removal by the reticuloendothelial system (RES). We have demonstrated that PEG-protected particles produced by Flash NanoPrecipitation using the block copolymers in this study have circulation times in mice of over 24 hours. 31 The ability to co-precipitate drugs in the same

nanoparticle makes it possible to formulate nanoparticle "drug cocktails" where multiple drugs can be released from the same nanoparticle in a dose-controlled and time-controlled manner. Our demonstration of tuned release of paclitaxel from these nanoparticles³¹ makes the combination of it with these NO-releasing compounds an ideal candidate for a dual drug delivery study. The paclitaxel release in our previous study could be tuned to release drug over times from 20 min to 24 h depending on the method of conjugation of the drug. This time scale could be matched to the 5–6 h release of PABA/NO.

Acknowledgments

This research was supported in part by the Intramural Research Program of the NIH, National Cancer Institute, Center for Cancer Research, as well as by National Cancer Institute contract HHSN261200800001E and the National Science Foundation under the NIRT grant for Nanoparticle Formation Technologies.

References

- Furchgott RF. Endothelium-Derived Relaxing Factor: Discovery, Early Studies, and Identification as Nitric Oxide (Nobel Lecture). Angew. Chem. Int. Ed 1999;38:1870–1880.
- Ignarro LJ. Nitric Oxide: A Unique Endogenous Signaling Molecule in Vascular Biology (Nobel Lecture). Angew. Chem. Int. Ed 1999;38:1882–1892.
- 3. Murad F. Discovery of Some of the Biological Effects of Nitric Oxide and Its Role in Cell Signaling (Nobel Lecture). Angew. Chem. Int. Ed 1999;38:1856–1868.
- 4. Keefer LK. Nitric Oxide (NO)- and Nitroxyl (HNO)-generating Diazeniumdiolates (NONOates): Emerging Commercial Opportunities. Curr. Top Med. Chem 2005;5:625–636. [PubMed: 16101424]
- Maciag A, Saavedra J, Chakrapani H. The Nitric Oxide Prodrug JS-K and Its Structural Analogues as Cancer Therapeutic Agents. Anticancer Agents Med. Chem 2009;9:798–803. [PubMed: 19538173]
- Kitagaki J, Yang Y, Saavedra JE, Colburn N, Keefer LK, Perantoni AO. Nitric Oxide Prodrug JS-K Inhibits Ubiquitin E1 and Kills Tumor Cells Retaining Wild-type p53. Oncogene 2009;28:619–624. [PubMed: 18978812]
- Simeone A-M, McMurtry V, Nieves-Alicea R, Saavedra J, Keefer L, Johnson M, Tari A. TIMP-2 Mediates the Anti-invasive Effects of the Nitric Oxide-releasing Prodrug JS-K in Breast Cancer Cells. Breast Cancer Res 2008;10:R44. [PubMed: 18474097]
- Chakrapani H, Kalathur RC, Maciag AE, Citro ML, Ji X, Keefer LK, Saavedra JE. Synthesis, Mechanistic Studies, and Anti-proliferative Activity of Glutathione/glutathione S-transferaseactivated Nitric Oxide Prodrugs. Bioorg. Med. Chem 2008;16:9764–9771. [PubMed: 18930407]
- 9. Chakrapani H, Goodblatt MM, Udupi V, Malaviya S, Shami PJ, Keefer LK, Saavedra JE. Synthesis and in vitro Anti-leukemic Activity of Structural Analogues of JS-K, an Anti-cancer Lead Compound. Bioorg. Med. Chem. Lett 2008;18:950–953. [PubMed: 18178089]
- 10. Kiziltepe T, Hideshima T, Ishitsuka K, Ocio EM, Raje N, Catley L, Li C-Q, Trudel LJ, Yasui H, Vallet S, Kutok JL, Chauhan D, Mitsiades CS, Saavedra JE, Wogan GN, Keefer LK, Shami PJ, Anderson KC. JS-K, a GST-activated Nitric Oxide Generator, Induces DNA Double-strand Breaks, Activates DNA Damage Response Pathways, and Induces Apoptosis in vitro and in vivo in Human Multiple Myeloma Cells. Blood 2007;110:709–718. [PubMed: 17384201]
- Udupi V, Yu M, Malaviya S, Saavedra JE, Shami PJ. JS-K, A Nitric Oxide Prodrug, Induces Cytochrome c Release and Caspase Activation in HL-60 Myeloid Leukemia Cells. Leuk. Res 2006;30:1279–1283. [PubMed: 16439016]
- 12. Shami PJ, Saavedra JE, Bonifant CL, Chu J, Udupi V, Malaviya S, Carr BI, Kar S, Wang M, Jia L, Ji X, Keefer LK. Antitumor Activity of JS-K [O2-(2,4-Dinitrophenyl) 1-[(4-Ethoxycarbonyl) piperazin-1-yl]diazen-1-ium-1,2-diolate] and Related O2-Aryl Diazeniumdiolates in Vitro and in Vivo. J. Med. Chem 2006;49:4356–4366. [PubMed: 16821795]
- 13. Liu J, Li C, Qu W, Leslie E, Bonifant CL, Buzard GS, Saavedra JE, Keefer LK, Waalkes MP. Nitric Oxide Prodrugs and Metallochemotherapeutics: JS-K and CB-3-100 Enhance Arsenic and Cisplatin Cytolethality by Increasing Cellular Accumulation. Mol. Cancer Ther 2004;3:709–714. [PubMed: 15210857]

14. Shami PJ, Saavedra JE, Wang LY, Bonifant CL, Diwan BA, Singh SV, Gu Y, Fox SD, Buzard GS, Citro ML, Waterhouse DJ, Davies KM, Ji X, Keefer LK. JS-K, a Glutathione/Glutathione S-Transferase-activated Nitric Oxide Donor of the Diazeniumdiolate Class with Potent Antineoplastic Activity1. Mol. Cancer Ther 2003;2:409–417. [PubMed: 12700285]

- 15. Ren Z, Kar S, Wang Z, Wang M, Saavedra JE, Carr BI. JS-K, A Novel Non-ionic Diazeniumdiolate Derivative, Inhibits Hep 3B Hepatoma Cell Growth and Induces c-Jun Phosphorylation via Multiple MAP Kinase Pathways. J. Cell. Physiol 2003;197:426–434. [PubMed: 14566972]
- 16. Townsend DM, Manevich Y, He L, Hutchens S, Pazoles CJ, Tew KD. Novel Role for Glutathione S-Transferase {pi}: Regulator of Protein S-Glutathionylation Following Oxidative And Nitrosative Stress. J. Biol. Chem 2009;284:436–445. [PubMed: 18990698]
- Andrei D, Maciag A, Chakrapani H, Citro ML, Keefer LK, Saavedra JE. Aryl Bis(diazeniumdiolates): Potent Inducers of S-Glutathionylation of Cellular Proteins and Their in Vitro Antiproliferative Activities. J. Med. Chem 2008;51:7944–7952. [PubMed: 19053760]
- 18. Townsend DM, Findlay VJ, Fazilev F, Ogle M, Fraser J, Saavedra JE, Ji X, Keefer LK, Tew KD. A Glutathione S-Transferase {pi}-Activated Prodrug Causes Kinase Activation Concurrent with S-Glutathionylation of Proteins. Mol. Pharmacol 2006;69:501–508. [PubMed: 16288082]
- 19. Saavedra JE, Srinivasan A, Buzard GS, Davies KM, Waterhouse DJ, Inami K, Wilde TC, Citro ML, Cuellar M, Deschamps JR, Parrish D, Shami PJ, Findlay VJ, Townsend DM, Tew KD, Singh S, Jia L, Ji X, Keefer LK. PABA/NO as an Anticancer Lead: Analogue Synthesis, Structure Revision, Solution Chemistry, Reactivity toward Glutathione, and in Vitro Activity. J. Med. Chem 2006;49:1157–1164. [PubMed: 16451080]
- Findlay VJ, Townsend DM, Morris TE, Fraser JP, He L, Tew KD. A Novel Role for Human Sulfiredoxin in the Reversal of Glutathionylation. Cancer Res 2006;66:6800–6806. [PubMed: 16818657]
- 21. Findlay VJ, Townsend DM, Saavedra JE, Buzard GS, Citro ML, Keefer LK, Ji X, Tew KD. Tumor Cell Responses to a Novel Glutathione S-Transferase-Activated Nitric Oxide-Releasing Prodrug. Mol. Pharmacol 2004;65:1070–1079. [PubMed: 15102935]
- 22. Chakrapani H, Wilde TC, Citro ML, Goodblatt MM, Keefer LK, Saavedra JE. Synthesis, Nitric Oxide Release, and Anti-leukemic Activity of Glutathione-activated Nitric Oxide Prodrugs: Structural Analogues of PABA/NO, an Anti-cancer Lead Compound. Bioorg. Med. Chem 2008;16:2657–2664. [PubMed: 18060792]
- Allen C, Maysinger D, Eisenberg A. Nano-engineering Block Copolymer Aggregates for Drug Delivery. Colloids Surf., B 1999;16:3–27.
- Kumar V, Prud'homme RK. Thermodynamic Limits on Drug Loading in Nanoparticle Cores. J. Pharm. Sci 2008;97:4904

 4914. [PubMed: 18300278]
- 25. Gref R, Minamitake Y, Peracchia M, Trubetskoy V, Torchilin V, Langer R. Biodegradable Long-circulating Polymeric Nanospheres. Science 1994;263:1600–1603. [PubMed: 8128245]
- 26. Schoenmakers RG, Wetering P. v. d. Elbert DL, Hubbell JA. The Effect of the Linker on the Hydrolysis Rate of Drug-linked Ester Bonds. J. Controlled Release 2004;95:291–300.
- 27. Patri AK, Kukowska-Latallo JF, Baker JR. Targeted Drug Delivery with Dendrimers: Comparison of the Release Kinetics of Covalently Conjugated Drug and Non-covalent Drug Inclusion Complex. Adv. Drug Deliv. Rev 2005;57:2203–2214. [PubMed: 16290254]
- 28. Kurtoglu YE, Navath RS, Wang B, Kannan S, Romero R, Kannan RM. Poly(amidoamine) Dendrimer-drug Conjugates with Disulfide Linkages for Intracellular Drug Delivery. Biomaterials 2009;30:2112–2121. [PubMed: 19171376]
- Perumal O, Khandare J, Kolhe P, Kannan S, Lieh-Lai M, Kannan RM. Effects of Branching Architecture and Linker on the Activity of Hyperbranched Polymer-Drug Conjugates. Bioconjugate Chem 2009:20:842–846.
- 30. Sengupta S, Eavarone D, Capila I, Zhao G, Watson N, Kiziltepe T, Sasisekharan R. Temporal Targeting of Tumour Cells and Neovasculature with a Nanoscale Delivery System. Nature 2005;436:568–572. [PubMed: 16049491]
- 31. Ansell SM, Johnstone SA, Tardi PG, Lo L, Xie S, Shu Y, Harasym TO, Harasym NL, Williams L, Bermudes D, Liboiron BD, Saad W, Prud'homme RK, Mayer LD. Modulating the Therapeutic

- Activity of Nanoparticle Delivered Paclitaxel by Manipulating the Hydrophobicity of Prodrug Conjugates. J. Med. Chem 2008;51:3288–3296. [PubMed: 18465845]
- 32. Saavedra JE, Srinivasan A, Bonifant CL, Chu J, Shanklin AP, Flippen-Anderson JL, Rice WG, Turpin JA, Davies KM, Keefer LK. The secondary amine/nitric oxide complex ion $R_2N[N(O)NO]^-$ as nucleophile and leaving group in S_N Ar reactions. J. Org. Chem 2001;66:3090–3098. [PubMed: 11325274]
- 33. Hillmyer MA, Bates FS. Synthesis and Characterization of Model Polyalkane-Poly(ethylene oxide) Block Copolymers. Macromolecules 1996;29:6994–7002.
- 34. Gindy ME, Ji S, Hoye TR, Panagiotopoulos AZ, Prud'homme RK. Preparation of Poly(ethylene glycol) Protected Nanoparticles with Variable Bioconjugate Ligand Density. Biomacromolecules 2008;9:2705–2711. [PubMed: 18759476]
- 35. Gindy ME, Panagiotopoulos AZ, Prud'homme RK. Composite Block Copolymer Stabilized Nanoparticles: Simultaneous Encapsulation of Organic Actives and Inorganic Nanostructures. Langmuir 2008;24:83–90. [PubMed: 18044945]
- 36. Johnson BK, Prud'homme RK. Chemical Processing and Micromixing in Confined Impinging Jets. AIChE J 2003;49:2264–2282.
- 37. Liu Y, Cheng C, Liu Y, Prud'homme RK, Fox RO. Mixing in a Multi-inlet Vortex Mixer (MIVM) for Flash Nano-precipitation. Chem. Eng. Sci 2008;63:2829–2842.
- 38. Akbulut M, Ginart P, Gindy ME, Theriault C, Chin KH, Soboyejo W, Prud'homme RK. Generic Method of Preparing Multifunctional Fluorescent Nanoparticles Using Flash NanoPrecipitation. Adv. Funct. Mater 2009;19:718–725.
- 39. Liu Y, Kathan K, Saad W, Prud'homme RK. Ostwald Ripening of Beta-Carotene Nanoparticles. Phys. Rev. Lett 2007;98:036102. [PubMed: 17358697]
- Kumar V, Wang L, Riebe M, Tung H, Prud'homme RK. Formulation and Stability of Itraconazole and Odanacatib Nanoparticles: Governing Physical Parameters. Mol. Pharmaceutics 2009;6:1118– 1124
- 41. Chen T, D'Addio SM, Kennedy MT, Swietlow A, Kevrekidis IG, Panagiotopoulos AZ, Prud'homme RK. Protected Peptide Nanoparticles: Experiments and Brownian Dynamics Simulations of the Energetics of Assembly. Nano Lett 2009;9:2218–2222. [PubMed: 19413305]
- 42. Molinspiration Cheminformatics. Bratislava, Slovak Republic: http://www.molinspiration.com/services/properties.html. Accessed on June 20, 2009
- 43. Liu J, Xiao Y, Allen C. Polymer-drug Compatibility: A Guide to the Development of Delivery Systems for the Anticancer Agent, Ellipticine. J. Pharm. Sci 2004;93:132–143. [PubMed: 14648643]
- 44. Daniels AU, Chang MKO, Andriano KP, Heller J. Mechanical Properties of Biodegradable Polymers and Composites Proposed for Internal Fixation of Bone. J. Appl. Biomater 1990;1:57–78. [PubMed: 10148987]
- 45. Matsumura Y, Maeda H. A New Concept for Macromolecular Therapeutics in Cancer Chemotherapy: Mechanism of Tumoritropic Accumulation of Proteins and the Antitumor Agent Smancs. Cancer Res 1986;46:6387–6392. [PubMed: 2946403]
- 46. Maeda H. SMANCS and polymer-conjugated macromolecular drugs: advantages in cancer chemotherapy. Adv. Drug Deliv. Rev 1991;6:181–202.
- 47. Maeda H, Sawa T, Konno T. Mechanism of tumor-targeted delivery of macromolecular drugs, including the EPR effect in solid tumor and clinical overview of the prototype polymeric drug SMANCS. J. Controlled Release 2001;74:47–61.

$$O_{0}$$
 O_{0} O_{0

Figure 1. Chemical structures of the diazeniumdiolate nitric oxide prodrugs used in this study.

Scheme 1. Glutathione-activated nitric oxide release from NO prodrug

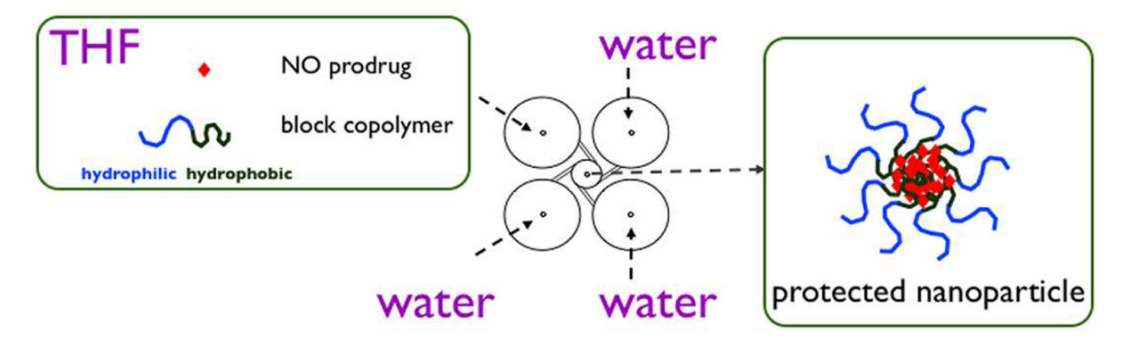


Figure 2.Schematic of nanoparticle formulation. Organic solvent stream, THF, is mixed with non-solvent, water, in a MIVM to precipitate the NO prodrug followed by stabilization with the block copolymers.

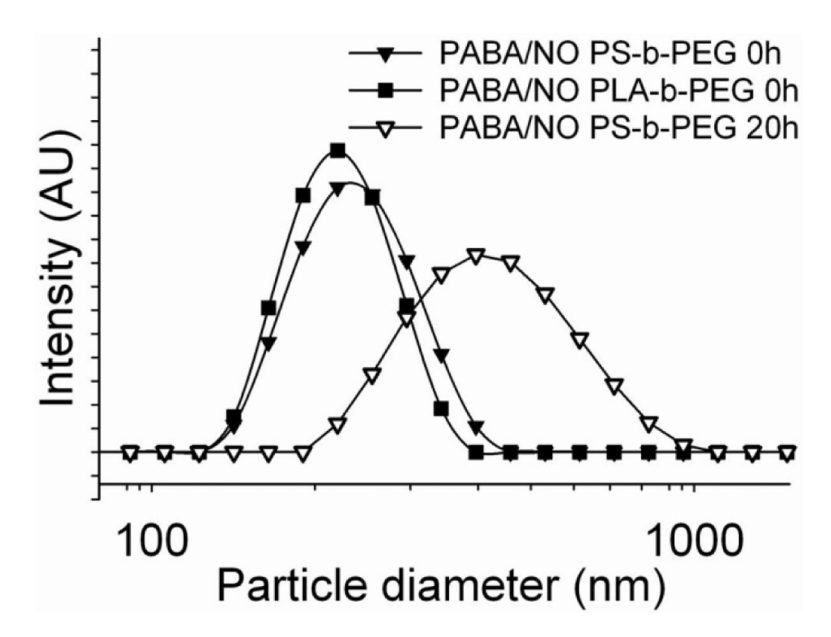


Figure 3. Particle size distributions of undialyzed PABA/NO nanoparticles stabilized by PS-*b*-PEG (240 nm) (▼) and PLA-*b*-PEG (225 nm) (■). The slow ripening of undialyzed nanoparticles stabilized by PS-*b*-PEG shows growth to 440 nm in 20 h (∇).

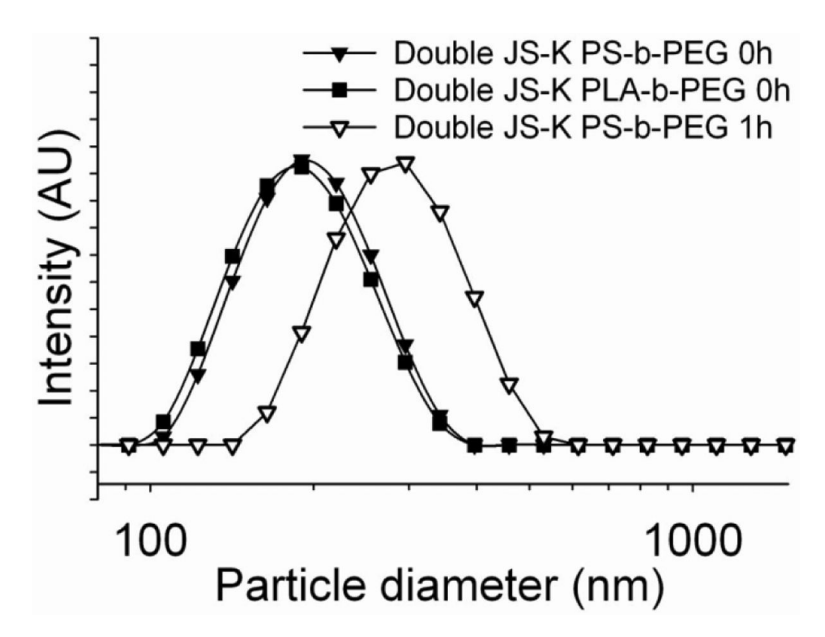


Figure 4. Particle size distributions of undialyzed Double JS-K nanoparticles stabilized by PS-*b*-PEG (200 nm) (▼) and PLA-*b*-PEG (195 nm) (■). The growth of the PS-*b*-PEG stabilized particles (to 290 nm) over 1 h is shown (∇).

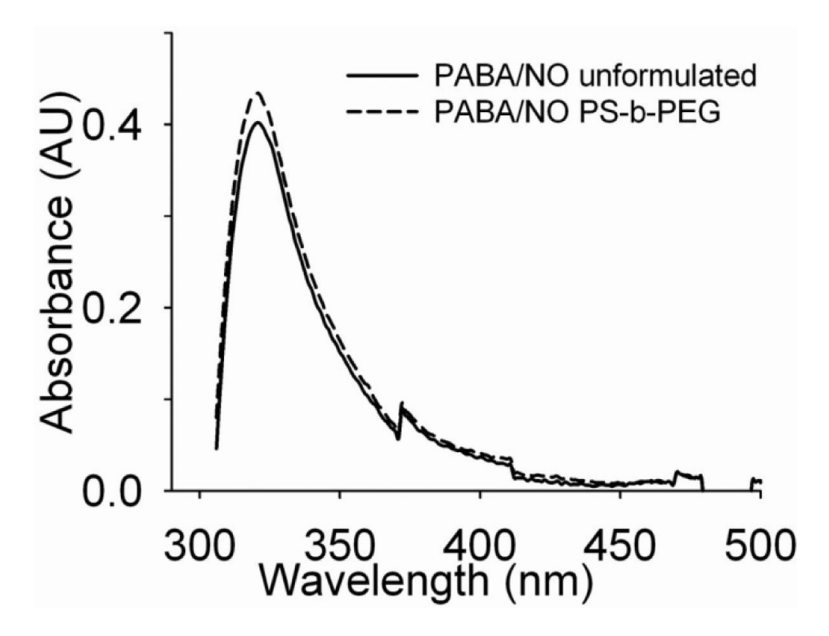


Figure 5.UV-vis absorbance spectra of formulated (stabilized by PS-*b*-PEG) vs unformulated PABA/NO. The spectra (peak position and intensity) confirm that molecular integrity is preserved during nanoparticle formation and lyophilization.

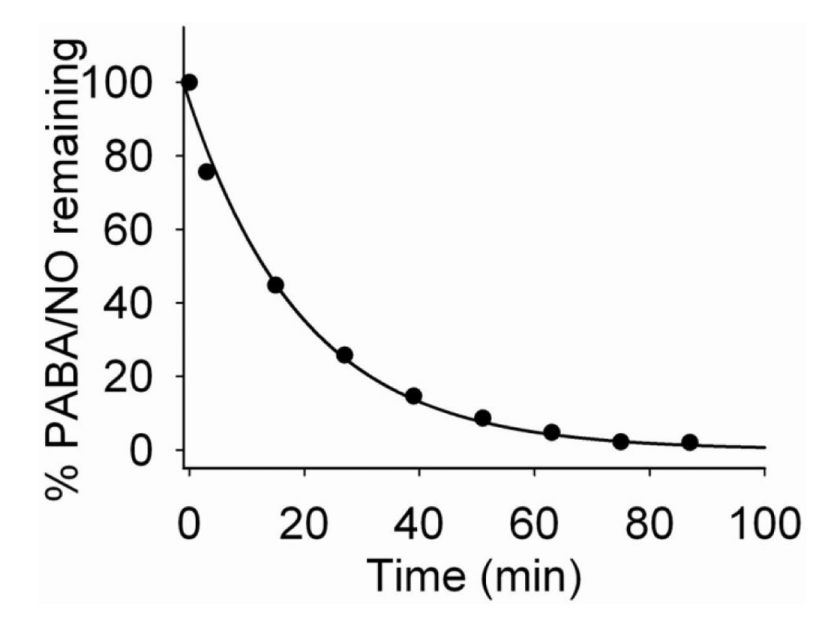


Figure 6. Decomposition of PABA/NO in 4 mM glutathione solution in pH 7.4 phosphate buffer at 25 °C.

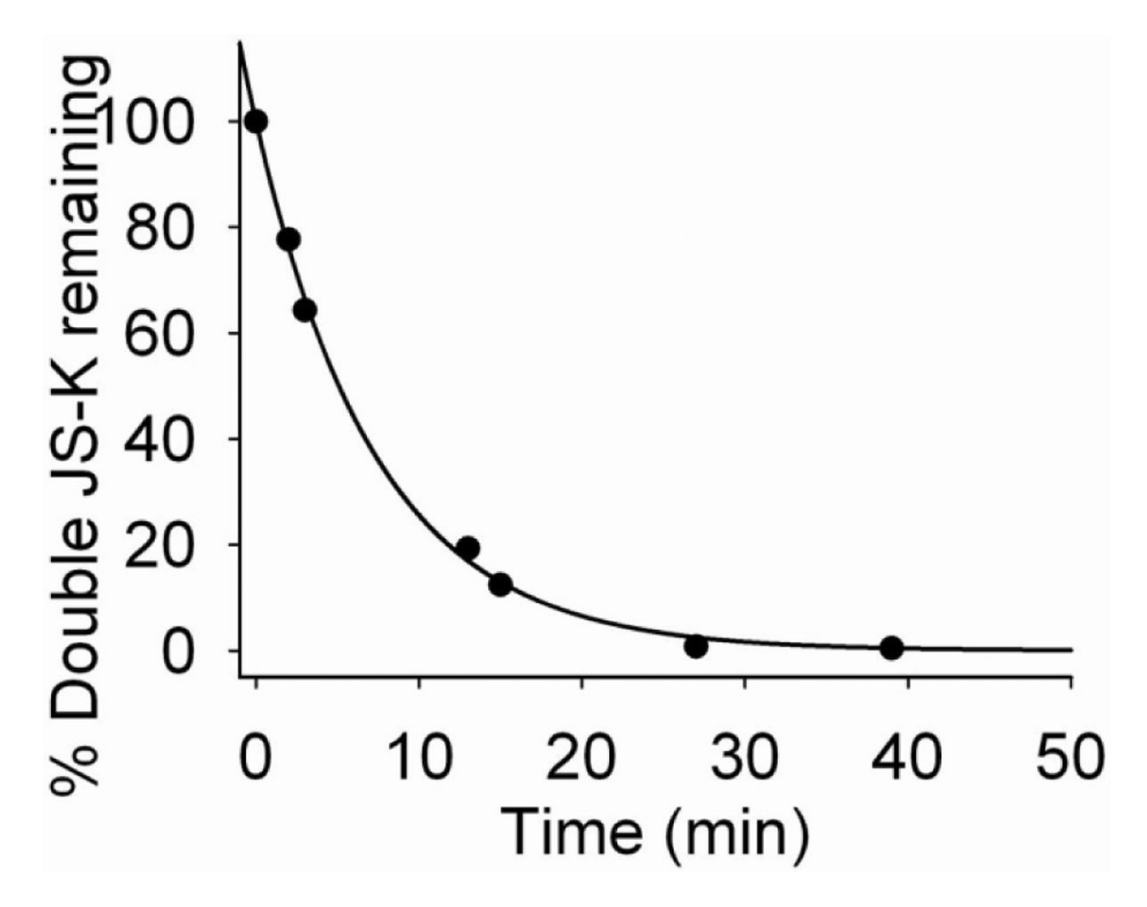


Figure 7. Decomposition of Double JS-K in 4 mM glutathione solution in pH 7.4 phosphate buffer at 25 °C.

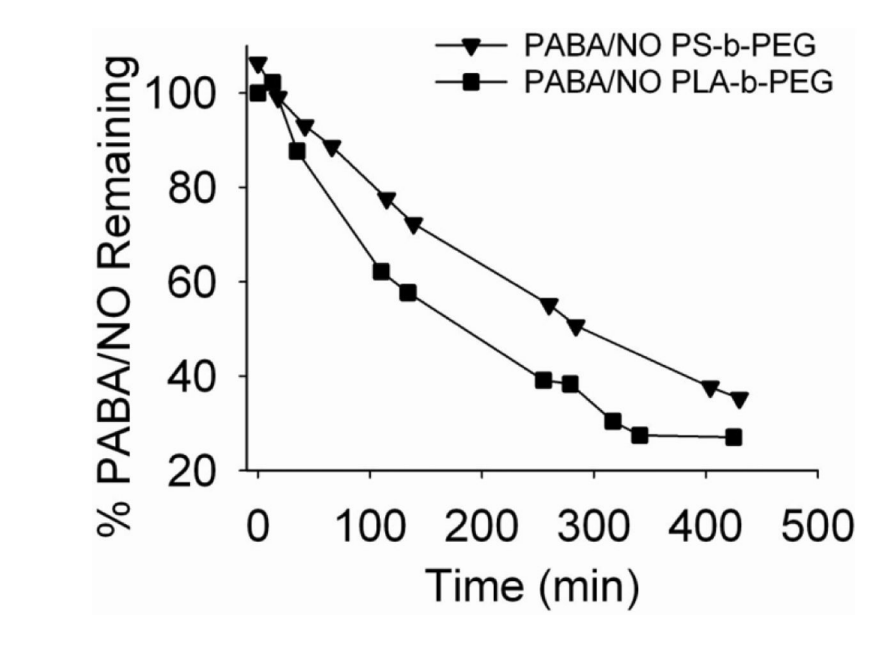


Figure 8. Decomposition of formulated PABA/NO in 4 mM glutathione solution in pH 7.4 phosphate buffer at 25 $^{\circ}$ C.

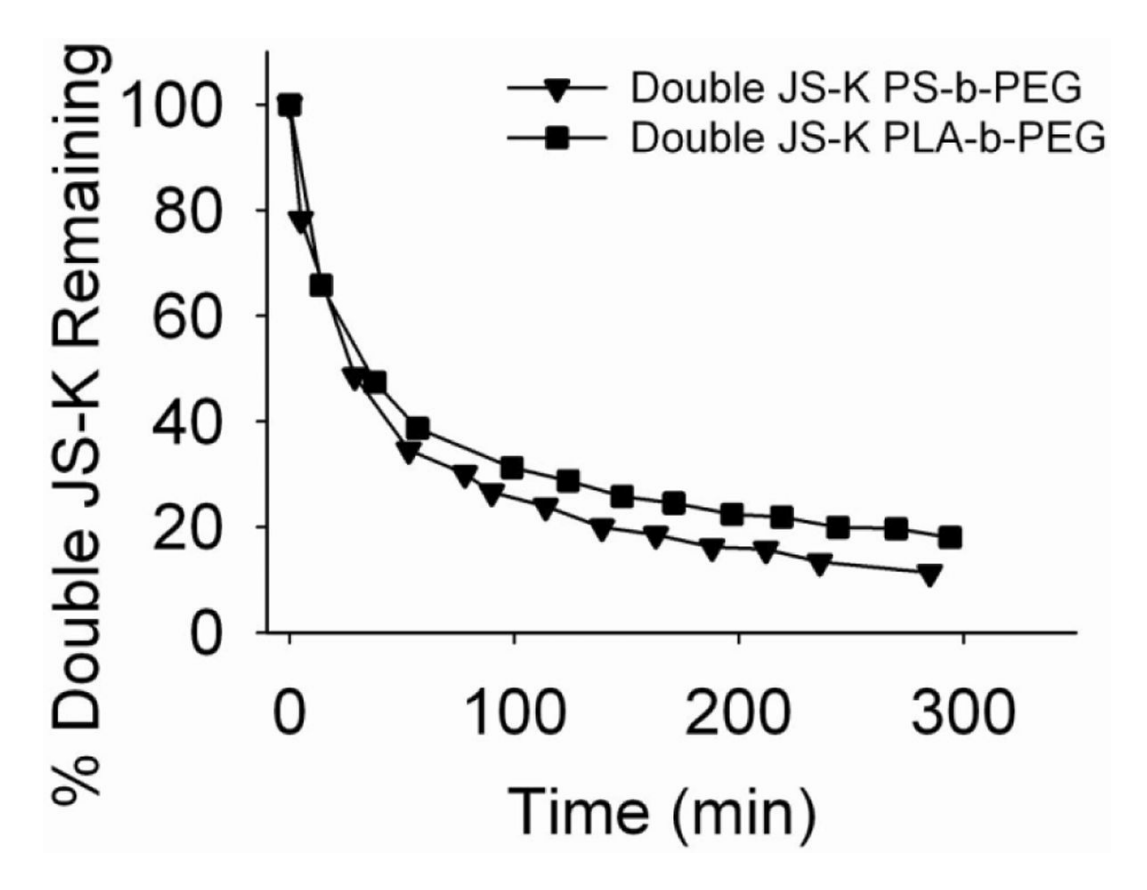


Figure 9. Decomposition of formulated Double JS-K in 4 mM glutathione solution in pH 7.4 phosphate buffer at 25 °C.

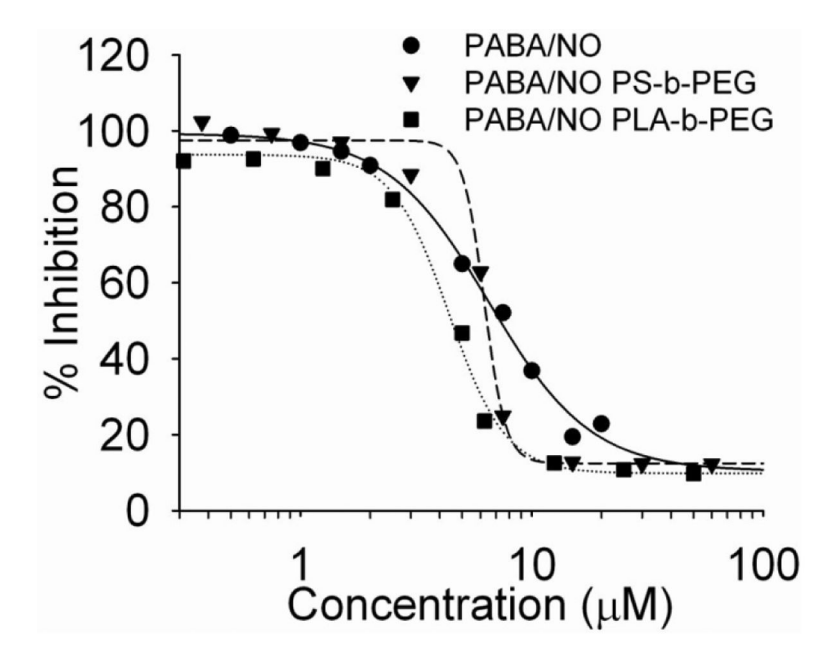


Figure 10. Anti-proliferative activity of PABA/NO, PS-*b*-PEG-stabilized PABA/NO and PLA-*b*-PEG-stabilized PABA/NO.

 Table 1

 Calculated recovery of PABA/NO and Double JS-K from their corresponding formulations

Compounds	Expected drug conc. (mg/mL) $\dot{\tau}$	Estimated drug conc. (mg/mL) for NP stabilized with ‡	
		PS-b-PEG	PLA-b-PEG
PABA/NO	0.27	0.23	0.22
Double JS-K	0.26	0.24	0.23

 $^{^{\}dagger}\textsc{Expected}$ drug concentration is based on the amount of drug used during the nanoparticle formulation.

 $^{^{\}ddagger}$ Estimated drug concentration is the actual drug content based on the HPLC analysis on formulated nanoparticles.

 $\label{eq:Table 2} \textbf{Anti-proliferative activities (IC}_{50}) \ of \ PABA/NO, \ PS-b-PEG \ stabilized \ PABA/NO \ \& \ PLA-b-PEG \ stabilized \ PABA/NO \$

Cell Lines	PABA/NO (μM)	PS-b-PEG-stabilized PABA/NO (μM)	PLA-b-PEG-stabilized PABA/NO (μM)
U937	6.5	5.0	4.4
H1703	8.7	6.3	5.3